Journal of the European Ceramic Society 16 (1996) 275–280

0955-2219(95)00156-5
0955-2219/96/$15.00

# Effects of Composition and Atmosphere on Reactive Metal Penetration of Aluminium in Mullite

Eduardo Saiz,[a] Antoni P. Tomsia,[a] Ronald E. Loehman[b] & Kevin Ewsuk[b]

[a]Center for Advanced Materials, Lawrence Berkeley Laboratory, Berkeley, CA, USA
[b]Sandia National Laboratories, Albuquerque, NM, USA

(Accepted 22 July 1995)

***Abstract***

*Ceramic–metal composites can be made by reactive penetration of dense ceramic preforms by molten Al. Molten Al will reduce mullite to produce a composite of $Al_2O_3$, Si and Al. The reaction can be written as $3Al_6Si_2O_{13} + (8 + x)Al \rightarrow 13Al_2O_3 + Al_xSi_y + (6 - y)Si$. The penetration is driven by the strongly negative Gibbs free energy for reaction. In order to assess the influence of atmosphere and temperature in the penetration process, reaction couples of molten Al on mullite were heated at temperatures from 950 to 1150°C, and at $p(O_2)$ from $\sim 10^{-10}$ to $\sim 10^{-20}$ atm. In this range $p(O_2)$ has little influence on reaction kinetics; the reaction rate is controlled by the rate of Si diffusion out of the preform to the external Al source.*

## Introduction

The development of ceramic/metal composites offers an opportunity to produce ceramics with significantly improved properties. Advanced ceramic composites are potential structural materials with improved strength, stiffness and toughness, and thus are more resistant to failure.[1,2]

Techniques for making ceramic/metal composites by reactive synthesis have been under development for a number of years. Processes that involve a gas-phase reactant include chemical vapour infiltration (CVI), gas-phase reaction bonding and the direct oxidation of molten metal.[3,4] Reactive processing of condensed phases to make composites include infiltration of reactive liquids into porous preforms, self-propagating high temperature synthesis (SHS) and *in situ* displacement reactions.[3–5]

Recently, several research groups have reported techniques for making ceramic/metal composites by reaction between molten metals and dense glass or ceramic preforms.[6–8] In these techniques, a dense oxide preform is converted to a composite as an oxidation–reduction reaction front moves into the preform. For example, reaction synthesis of composites in the $SiO_2$/Al system has recently been reported by Matsuo and Inabe[6] and by Breslin *et al.*[7,8] Matsuo and Inabe[6] made $Al_2O_3$/Al/Si composite bodies by reacting amorphous silica and molten aluminum at 900–1000°C. The reaction product was a mutually interpenetrating structure of ~70 wt% alumina and ~25 wt% Al with reported improvements on bend strength and other physical properties. Breslin *et al.*[7,8] also reacted amorphous silica with molten aluminium to give similar composites.

In contrast to the work just cited, the ceramic–metal composites discussed in this paper are synthesized from dense ceramic preforms rather than from amorphous silica. Al reacts and penetrates dense ceramic mullite preforms according to the reaction:

$$3(3Al_2O_3{\cdot}2SiO_2) + (8 + x)Al \rightarrow 13Al_2O_3 + Al_xSi_y + (6 - y)Si \quad (1)$$

The reaction product has the form of an interpenetrating diphasic composite of alumina and an Al/Si alloy (Fig. 1). The reactive metal penetration technique has the advantage of producing complex ceramic parts with near net-shape and very low porosity. It appears that the mechanism for reactive penetration of polycrystalline ceramics such as mullite[9,10] is completely different from that for the glass preforms described above.[6–8] Thus the method discussed in this paper can be expected to have its own specific advantages for synthesis of ceramic/metal composites.

If reactive metal penetration is to be a commercially useful way of composite fabrication, it must be economical, reliable and designed to produce the adequate microstructures that will optimize critical properties. The main objective of this work was to study the processing variables that affect Al wetting and reaction with mullite substrates, with particular emphasis on the effects of temperature and $p(O_2)$.

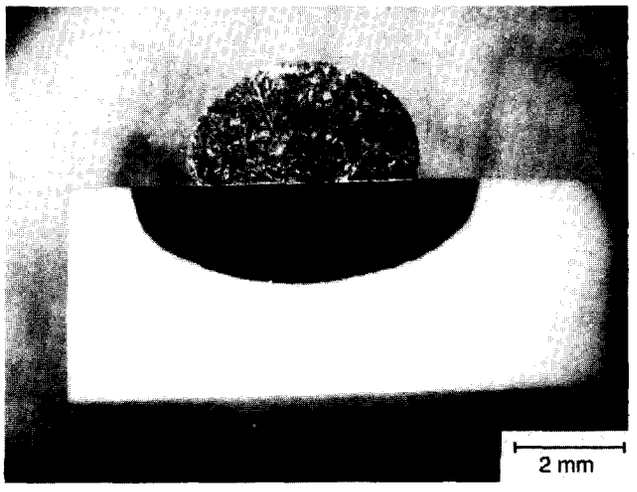


(a)

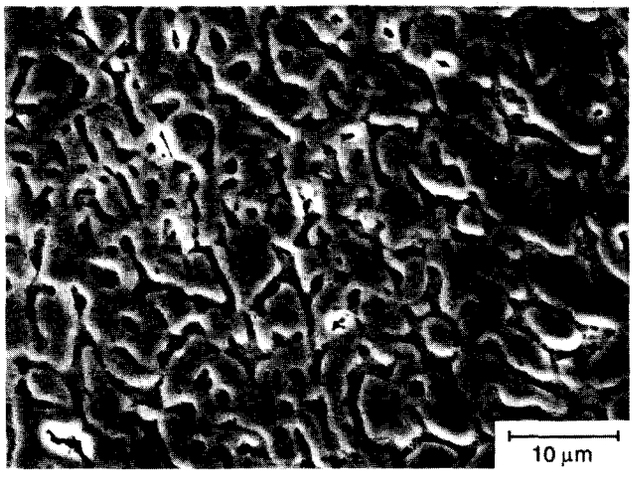


(b)

**Fig. 1.** (a) Al drop on mullite substrate after reaction for 60 min at 1100°C. The reaction zone under the Al drop is a composite of Al and $Al_2O_3$. (b) Micrograph of the composite reaction zone showing the interpenetrating $Al/Al_2O_3$ microstructure.

## Experimental

Mullite substrates for the wetting and infiltration experiments were made using Chichibu MP40 mullite powder (Scimarec Co., Ltd., Tokyo, Japan). Mullite ceramic pellets were formed by cold isostatic pressing at ~200 MPa and sintering in vacuum (~$6{\cdot}7 \times 10^{-4}$ Pa) at 1600–1650°C for 2 h. The final compacts (~200 g) had a density $\rho \geq 95\%$ theoretical. Mullite substrates (~$2 \times 2 \times 0{\cdot}5$ mm) were cut using a diamond saw and were subsequently surface finished using a 800 grit resin-bonded diamond wheel.

Contact angle measurements of molten Al on mullite were made by placing Al cylinders (0·2–0·3 g) on the substrates, and the assemblies were heated in 30 min to the test temperature (950–1150°C) in a furnace with a tubular metal resistance heating element. The contact angle was monitored through a porthole in the furnace and recorded as a function of time using a telegoniometer. The temperature was recorded with a calibrated Pt–Pt10Rh thermocouple. After the test, the sample was cooled in 10 min to 900°C and in 300 min from 900°C to room temperature. Al/Si alloys for wetting studies were made *in situ* by placing Si chips over the Al cylinders.

The tests were performed in two kinds of atmospheres.

(a) High $p(O_2)$: Ar (99·998%) flow (0·5 l $min^{-1}$) with a Pt tube resistance heating element, $p(O_2)$ ~$10^{-10}$ atm.

(b) Low $p(O_2)$: Ar (99·998%) gettered with Ti/Zr chips at 900°C, flowing (0·5 l $min^{-1}$) with a Ta tube resistance heating element lined inside with Zr foil, $p(O_2)$ ~$10^{-20}$ atm.

In both cases the $p(Ar)$ was kept slightly higher than 1 atm.

After the tests, the samples were mounted in an epoxy resin and cut perpendicular to the metal/ceramic interface. The cross-sections were then polished to 1/4 μm diamond finish. The thickness and volume of the reaction layer and its microstructure were measured using reflected light optical microscopy (RLOM) and scanning electron microscopy (SEM). Elemental analysis and X-ray mapping were performed both by energy dispersive (EDS) and wavelength dispersive (WDS) methods.

## Results and Discussion

Figure 2 shows the contact angles and reaction layer thicknesses vs. time for wetting experiments carried out at 1100°C, for times up to 150 min in both high and low $p(O_2)$ atmospheres. In the high $p(O_2)$ atmosphere (~$10^{-10}$ atm) a thick oxide layer developed on the surface of the Al drop, making the contact angle measurement unreliable. In low $p(O_2)$ (~$10^{-20}$ atm) the drop surface was shinier and measurements were reproducible. Even after 150 min an equilibrium contact angle was not reached. Despite the differences in contact angles, the microstructures and thicknesses of the reaction layers were practically the same for both atmospheres. The microstructure is that of an $Al_2O_3$–Al/Si (alloy) composite. The reaction layer thickness did not follow a $t^{1/2}$ law as would be expected for a diffusion driven process (Fig. 2).

Contact angle measurements carried out for 60 min at temperatures ranging from 950 to 1150°C in low $p(O_2)$, Fig. 3, show an equilibrium contact angle value of 140° at 950°C. At 1000°C there is a sudden decrease, from ~140° to ~110°, after 25–30 min. For higher temperatures the contact angle decreases with time to values down to ~90°. Measurements of the reaction layer thickness after

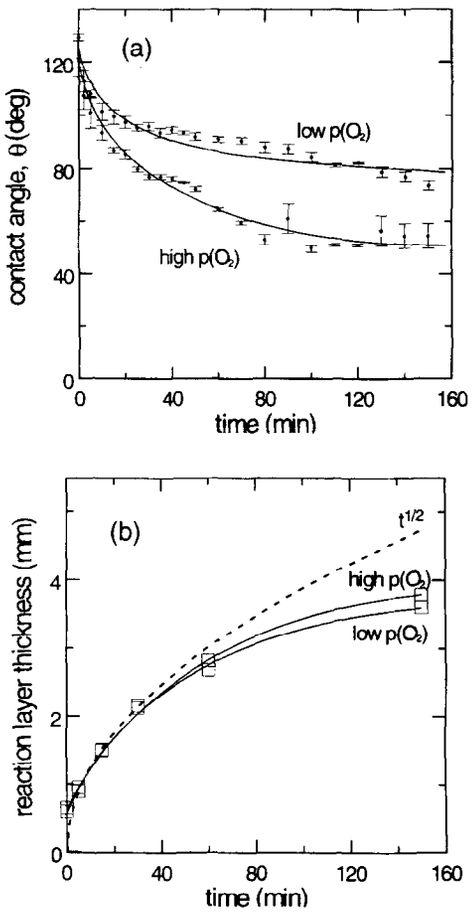


**Fig. 2.** (a) Contact angle vs. time for aluminium on mullite in different atmospheres ($T$ = 1100°C). (b) Reaction layer thickness vs. time after the wetting experiments ($T$ = 1100°C).

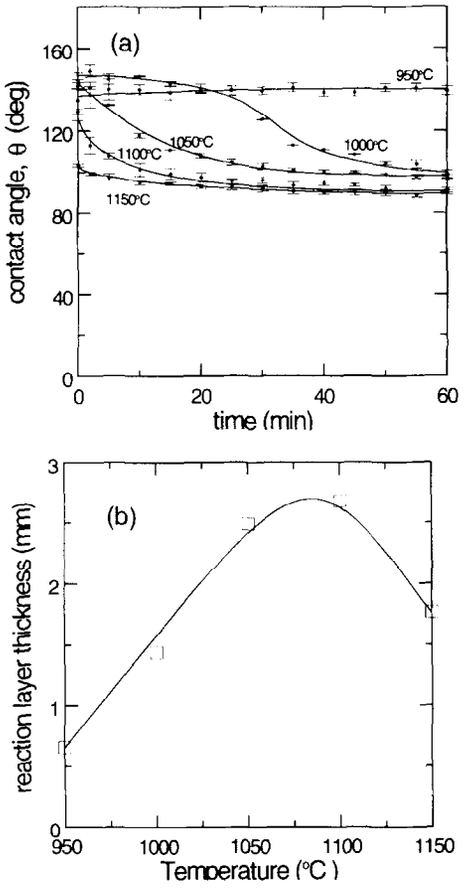


**Fig. 3.** (a) Contact angle vs. time at different temperatures for Al on mullite at low $p(O_2)$. (b) Reaction layer thickness after wetting experiments at different temperatures in a low $p(O_2)$ atmosphere.

the experiments show a maximum around 1100°C (Fig. 3).

Si mapping and EDS analysis in the reaction layer revealed a lower Si content than that corresponding to the original mullite substrate (Fig. 4). This decrease is due to Al–Si interdiffusion during the test. Large silicon crystals can be observed in the drop (darker crystals in Fig. 5) and metallic Al/Si alloy in the reaction layer after the experiment. There is a small gradient in the Si content in the reaction layer, reaching a maximum at the interface between reaction layer and mullite. The Si content at that interface increases with time at the reaction temperature (Fig. 4).

Wetting experiments between pure Al and mullite were also performed using larger Al drops. In Fig. 6 it can be observed that when the test is done using a 1·43 g drop the contact angle is larger than the one corresponding to the small drops (0.2–0.3 g), and the reaction layer is thicker with the larger Al drop. The thicknesses corresponding to reactions for 0, 5 and 15 min with the small drop and 150 min with the big one fit to a $t^{1/2}$ law.

In order to further assess the role of Al–Si interdiffusion and Si dissolution into Al, a wetting experiment was carried out at 1100°C in a low $p(O_2)$ atmosphere using a Al/Si (40/60 wt%) liquid alloy already saturated with silicon at the test temperature (saturation value at 1100°C is 56 wt% Si[11]). The contact angle of the Al/Si alloy reached an equilibrium value of 55° (Fig. 6) and the corresponding reaction layer thickness is 180 $\mu$m (~20 times smaller than for pure Al).

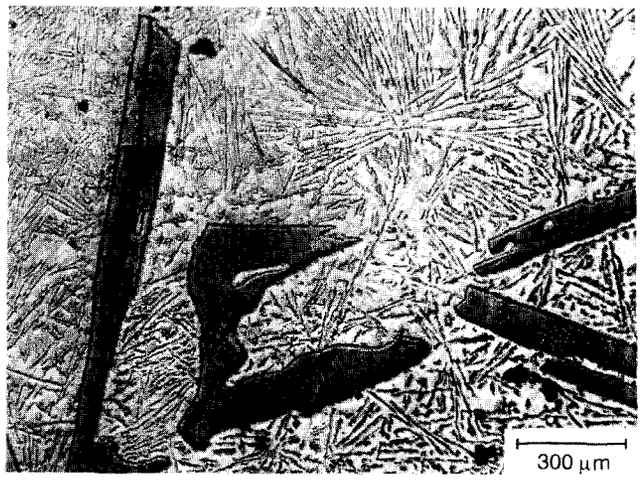


**Fig. 4.** Micrograph of Al drop after reacting with mullite substrate for 60 min at 1100°C. The needle-like crystals are from Si that diffuses into the molten Al drop during reaction.

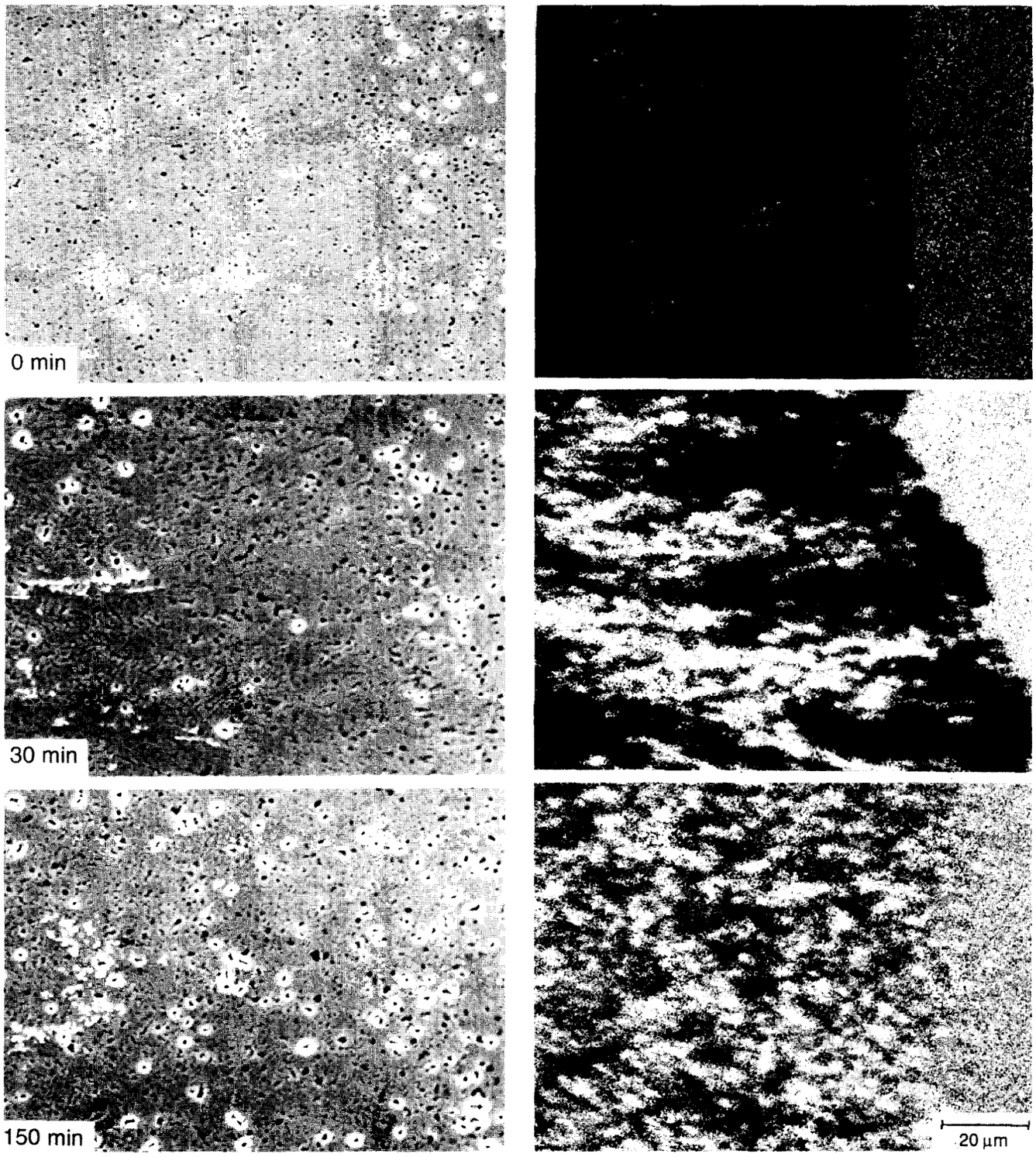


**Fig. 5.** Micrographs of interface between $Al/Al_2O_3$ composite and unreacted mullite after 0, 30 and 150 min at 1100°C. The right-hand photos are X-ray compositional maps of Si.

**Table 1.** Free energy values corresponding to Eqns (3) and (5), $y$ (wt%) value corresponds to Si saturation at each temperature, $\Delta G_2$ is calculated taking $N = 6/y$ (Refs 13 and 14).

| *Temperature* (°C) | $\Delta G_1$ (*kJ*) | y (*Si solubility in Al*)[11] | $\Delta G_2$ (*kJ*) | $\Delta G_R$ (*kJ*) |
|---|---|---|---|---|
| 950 | −952 | 0·42 | −46 | −998 |
| 1000 | −933 | 0·46 | −44 | −977 |
| 1050 | −914 | 0·52 | −39 | −953 |
| 1100 | −895 | 0·56 | −35 | −930 |
| 1150 | −876 | 0·62 | −29 | −905 |

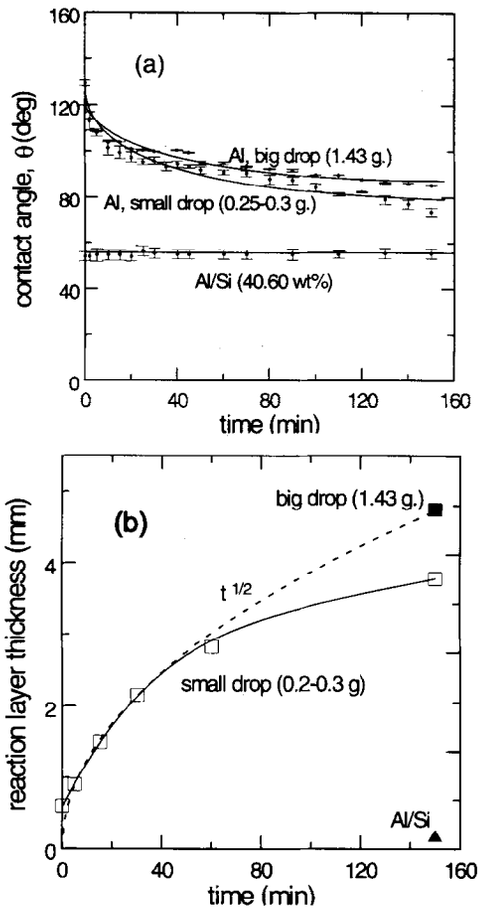


**Fig. 6.** (a) Contact angle vs. time for different sizes of Al drop and Al/Si alloy on mullite. (b) Corresponding reaction layer thicknesses.

As has been reported by Brennan and Pask,[12] under most conditions there is always an $Al_2O_3$ layer present on the surface of aluminium. Those authors report that temperatures higher than 950–1000°C are necessary to break that layer and expose fresh Al to the furnace atmosphere. This effect could explain the invariant contact angle of Al on mullite at 950°C in low $p(O_2)$, see Fig. 3. The sudden decrease in contact angle at 1000°C is probably related to the breakup of this alumina layer.

At $T \leq 1000$°C the presence of an $Al_2O_3$ passivating layer on the metal drop surface inhibits the contact of fresh Al and the mullite substrate, consequently reduced reaction rates are observed (Fig. 3). At $T > 1000$°C, and once the passivating layer breaks, fresh Al is in contact with the ceramic; the reaction front seems isolated from the furnace atmosphere and reaction kinetics together with reaction layer microstructure and composition do not depend on $p(O_2)$ (Figs 3 and 4).

At the test temperature, the net reaction (1) between mullite and Al can be rewritten to show the effect of the starting amount of Al on Si precipitation:

$$3(3Al_2O_3{\cdot}2SiO_2)\{s\} + (8 + Nx)Al\{1\} \rightarrow 13Al_2O_3\{s\} + NAl_xSi_y\{1\} + (6 - Ny)Si\{s\} \quad (2a)$$

where $x + y = 1$ and where $y$, the solubility of Si in Al, depends on temperature. $Nx$ represents the excess of Al with respect to the amount necessary for mullite reduction.

With an excess of Al (no Si precipitates, $N > 6/y$):

$$3(3Al_2O_3{\cdot}2SiO_2)\{s\} + (8 + Nx)Al\{1\} \rightarrow 13Al_2O_3\{s\} + NAl_xSi_{6/N}\{1\} \quad (2b)$$

$\Delta G_R$, the change in free energy corresponding to the reactions (2a) and (2b), must be negative in order for the reactions to proceed as written.

The reactions (2a) and (2b) are made up of two partial reactions, Eqns (3) and (4a), (4b):

$$3(3Al_2O_3{\cdot}2SiO_2)\{s\} + 8Al\{1\} \rightarrow 13Al_2O_3\{s\} + 6Si\{s\} \qquad \Delta G_1 \quad (3)$$

The second partial reaction can be written in two ways, depending on whether the Si concentration is high enough to give precipitates. For $N \leq 6/y$ [Eqn (2a)], Si precipitates:

$$Nx Al\{1\} + 6Si\{s\} \rightarrow NAl_xSi_y\{1\} + (6 - Ny)Si\{s\} \qquad \Delta G_2 \quad (4a)$$

For $N > 6/y$ [Eqn (2b)], no Si precipitates:

$$Nx Al\{1\} + 6Si\{s\} \rightarrow NAl_xSi_{6/N}\{1\} \quad \Delta G_3 \quad (4b)$$

Then, depending on whether the concentration of Si exceeds the solubility limit at the processing temperature or not:

$$\Delta G_R = \Delta G_1 + \Delta G_2 \quad \text{or} \quad \Delta G_R = \Delta G_1 + \Delta G_3 \quad (5)$$

Table 1 shows some of the $\Delta G_R$, $\Delta G_1$, $\Delta G_2$ and $y$ values at different temperatures. It can be seen that the contribution of Si dissolution to the total free energy of the reaction is relatively low.

The corresponding change in the volume of solids at the test temperature is:

$$\%\Delta V = [13V_{Al2O3} + (6 - Ny)V_{Si} - 3V_{3Al2O3{\cdot}2SiO2}] \times 100/3V_{3Al2O3{\cdot}2SiO2} \quad (6)$$

where $V_{Al2O3}$ (25·7 cm$^3$ mol$^{-1}$), $V_{Si}$ (12·1 cm$^3$ mol$^{-1}$) and $V_{3Al2O3{\cdot}2SiO2}$ (135 cm$^3$ mol$^{-1}$) are correspondingly the molar volumes of alumina, silicon and mullite. If the liquid does not dissolve any of the Si that originates from the mullite reduction, $y = 0$ and $\%\Delta V \approx 0$, Al and mullite must then react by solid-state diffusion through an $Al_2O_3$/Si layer. On the other hand, if there is a Si dissolution, $y > 0$ and $\%\Delta V < 0$ ($\%\Delta V = -17\%$ for $y = 6/N$), space is created through which the Al/Si liquid can penetrate into the reaction front and the reaction can progress at a faster pace than the one corresponding to solid-state diffusion driven processes. When the experiment is performed using Al/Si alloy already saturated in Si, the liquid does not dissolve any silicon coming from mullite reduction; then, on one hand, there is a reduction in the total free energy of the reaction because the inverse of Eqn

(4a), for $N = 6/y$, takes place, while on the other hand, the liquid does not dissolve Si and does not create space to penetrate fast into the reaction front. These can explain the lower reaction rate observed for the Al saturated with Si at the test temperature (Fig. 6).

In the case of the small drop, the concentration of Si in the Al drop increases noticeably after 30–60 min, consequently the diffusion rate of Si decreases and so does the reaction rate. In the case of the large drop the Si concentration remains low and the diffusion rate of Si remains constant, consequently the reaction rate is higher and exhibits a $t^{1/2}$ law corresponding to a diffusion-driven process. The calculated diffusion coefficient, $D \approx 2 \times 10^{-5}$ cm$^2$ s$^{-1}$, is in the order of diffusion coefficients observed in liquid metals.[15]

These results indicate that Si/Al interdiffusion is the kinetic limiting step for the reaction/penetration of molten Al into dense mullite ceramics.

It can also be observed that the contact angle does not decrease when the reaction layer thickness increases (the bigger drop has a bigger reaction layer). It seems that the decrease in contact angle as the reaction goes on is more related to the increase in Si concentration in the drop.

## Conclusions

The results presented in this paper indicate that the kinetic limiting step for the reactive penetration of molten Al into dense mullite substrates is the diffusion of Si out of the composite. In the range of $p(O_2)$ studied the oxygen partial pressure does not affect appreciably either the penetration rate or the microstructure of the reaction layer.

These data suggest that processing conditions can be adjusted to make this a practical system for the fabrication of metal/ceramic composites by reactive metal penetration.

## Acknowledgements

This work was supported by the US DOE Office of Industrial Technologies and the US DOE under contract No. DE-AC04-94AL85000. E. Saiz wishes to acknowledge Fulbright Foundation and MEC (Spain) for financial support.

## References

1. Harrigan, W. C. Jr, in *Metal Matrix Composites Processing and Interfaces*, eds R. K. Everett & R. J. Arsenault, Academic Press, New York, 1991, Vol. 1.
2. Ashby, M. F., *Acta Metall. Mater.*, **41**[5] (1993) 1313.
3. Chiang, Y., Haggerty, J. S., Messner, R. P. & Demetry, C., *Ceram. Bull.*, **68**[2] (1989) 420.
4. Claussen. N., *J. de Physique IV, Colloque C7*, **3** (1993) 1327.
5. Hilling, W. B., *Ceram. Bull.*, **73**[4] (1994) 56.
6. Matsuo, S. & Inabe, T., *Tokyo Ceramics*, (1991) 222.
7. Breslin, M. C., Rignalda, J., Seeger, J., Marasco, A. L., Daehn, G. S. & Fraser, H. L., *Ceram. Eng. Sci. Proc.*, **15**[4] (1994) 104.
8. Breslin, M. C., US Pat. No 5 214 011, 25 May 1993.
9. Tomsia, A. P., Loehman, R. E. & Ewsuk, K., *J. Am. Ceram. Soc.*, submitted.
10. Fahrenholtz, W. G., Ewsuk, K. G., Loehman, R. L. & Tomsia, A. P., in *In Situ Reactions for Synthesis of Composites, Ceramics and Intermetallics*, eds E. B. Berrera, F. D. S. Marquis, W. E. Frazier, S. G. Fishman, N. N. Thadhani & Z. A. Munir, The Minerals, Metals and Materials Society, Warrendale, PA, 1995.
11. *Binary Alloy Phase Diagrams*, ed. T. B. Massalski, ASM International, Metals Park, OH, 1990.
12. Brennan, J. J. & Pask, J. A., *J. Am. Ceram. Soc.*, **51**[10] (1968) 569.
13. Kubachesvsky, O. & Alcock, C. B. (eds), *Principles of Metallurgical Thermodynamics, 5th Edn*, Pergamon Press, New York, 1979.
14. HSC Chemistry for Windows, Outokumpu Research.
15. Smithells, C. J. (ed.), *Metals Reference Book*, Butterworth & Co, London, 1976.